



## Observations of the Dimensional Stability of Four GCL Products under Combined Thermal and Moisture Cycles

L.E. Bostwick, GeoEngineering Centre at Queen's-RMC, Queen's University, Kingston, Canada  
R.K. Rowe, GeoEngineering Centre at Queen's-RMC, Queen's University, Kingston, Canada  
W.A. Take, GeoEngineering Centre at Queen's-RMC, Queen's University, Kingston, Canada  
R.W.I. Brachman, GeoEngineering Centre at Queen's-RMC, Queen's University, Kingston, Canada

### ABSTRACT

To investigate the possibility that combined thermal and moisture cycles can cause irrecoverable shrinkage of geosynthetic clay liner (GCL) panels when left exposed in the field, the dimensional stability of four different GCL products were investigated under idealised cycles in the laboratory. A number of variables, including type of GCL, initial moisture content and boundary conditions were examined to assess the effects of these variables on the potential incremental and total shrinkage. Nine samples, involving four different GCL products were tested to investigate whether the specific characteristics of each GCL had an effect on the observed GCL shrinkage. The resulting deformations of the panels were then measured using both hand measurements and digital image correlation techniques. These preliminary results indicate that cyclical shrinkage of GCLs is anisotropic, and that different products shrink at different rates and to different final magnitudes.

### 1. INTRODUCTION

Geosynthetic Clay Liners (GCLs) are often used beneath a geomembrane to form a composite liner system in modern waste containment facilities. Typically, the geomembrane is placed directly over the GCL. If there are no holes in the geomembrane, fluid is unable to pass through the geomembrane under a hydraulic gradient. However, if a hole is present, the GCL greatly reduces the amount of leakage (Rowe 2005). GCLs are delivered as rolls of panels approximately 4.7m wide. The panels are placed adjacent to each other with an overlap between panels.. This overlap, which is typically 0.15 to 0.3m, is often lined with powdered bentonite to further seal the seam. However, an number of recent exhumations of field installations which have been subjected to extreme exposure conditions revealed the overlap was eliminated, and gaps of between 200 and 1200mm had formed between adjacent panels (Thiel and Richardson, 2005; Koerner and Koerner, 2005).

Shrinkage across the panel width induced by cyclic wetting and drying was suggested as a possible basis for the observed field shrinkage, with the cyclic behavior being caused by temperature variations related to solar radiation on an exposed geomembrane, (Thiel and Richardson, 2005; Koerner and Koerner, 2005). Laboratory tests using tap water as the wetting fluid (Thiel et al., 2006, Bostwick et al., 2007) have clearly shown that combined thermal and moisture cycles result in panel shrinkage, however, the exact mechanism by which this occurs remains unclear. The relationship between shrinkage and several variables, such as type of GCL and testing boundary conditions, are of particular interest. The objective of this paper is to present preliminary results on the influence of these factors on potential GCL shrinkage.

### 2. FIELD WETTING AND DRYING

In the field, GCLs are typically installed at their as-manufactured water content. Depending on the manufacturer and the method of fabrication, this moisture content can range from 5% up to approximately 25-30%; certain products may even be as high as 36% coming off the roll. Following installation, the GCL hydrates by drawing moisture from the underlying foundation soil. As the water content of the GCL increases, it causes the material to swell. The hydraulic conductivity decreases, allowing it to perform its function as a moisture barrier.

At some sites, the geomembrane may be left exposed for an extended period of time. If this occurs, allowing the geomembrane to be exposed to daily thermal cycles, its temperature will increase, thereby heating the GCL. Geomembrane temperatures of up to 70°C (Pelte et al., 1994; Koerner and Koerner, 1995) have been recorded. As heat is transferred to the GCL, it is subjected to a drying cycle. The moisture lost may either be driven back into the foundation soil, or it may collect at the interface between the geomembrane and the GCL, particularly at locations where a gap exists between the two (for example, at a geomembrane wrinkle). If the liner is located on a slope, the moisture has the potential to flow downslope, resulting in overall GCL moisture loss at the location in question.

As solar radiation decreases, (usually corresponding to the decrease in temperature occurring at the end of the day) the GCL rehydrates. This can occur in the same manner as the initial hydration, with the GCL drawing moisture from the

foundation soil; the GCL may also reabsorb some of the water from the gap between the geomembrane and the GCL. As the temperature of the geomembrane fluctuates daily, the GCL may undergo multiple wetting and drying cycles.

### 3. PREVIOUS WORK ON GCL SHRINKAGE

Koerner and Koerner (2005) and Thiel et al. (2006) have shown that, on a scrim-reinforced GCL, monotonic drying does not result in shrinkage strains sufficiently large to explain the loss of overlap observed at the field sites. Similarly, cyclic wetting and drying of the geotextile component of a GCL product produces negligible shrinkage (Thiel et al., 2006).

Thiel et al. (2006) conducted a number of laboratory tests examining GCL shrinkage. They concluded that specimens with nonwoven/nonwoven geotextiles tended to experience greater shrinkage than those comprised of a nonwoven/woven combination; they also found that adding a greater volume of water to the sample during the hydration phase resulted in higher shrinkage. It was suspected that a lower initial water content would result in a comparatively lower quantity of shrinkage.

Bostwick et al (2007) studied the effect of size and aspect ratio on potential GCL shrinkage. In this study, it was shown that the size of the specimen in question did not affect the magnitude of shrinkage observed. However, aspect ratio was found to influence shrinkage, with larger aspect ratios (i.e. 10:1, 5:1) experiencing greater shrinkage than those which were smaller (i.e. 1.7:1, 1:1).

Brachman et al. (2007) constructed a 40m x 80m experimental GM/GCL site at Godfrey, Ontario, to assess the effect of daily thermal cycles experienced by an uncovered GM/GCL liner. The site is also intended to address the dimensional stability of GCL panel overlaps.

### 4. TEST SPECIMENS

Four different GCLs were selected for this study. A description of the GCLs is given in Table 1. A total of nine GCL samples from a variety of types of GCL were tested to investigate their possible shrinkage. The tests also examined the effect of boundary conditions. The test samples, as well as their initial properties, are summarized in Table 2.

Table 1 – Properties of Selected GCLs as they normally come off the roll in the field

GCL	Manufacturer	Lower GT	Upper GT	GCL Mass (g/m <sup>2</sup> )	Layer Connection
GCL 1	A	Woven slit-film (W)	Nonwoven needle-punched (NW)	5460	Needle-punched, thermally treated
GCL 2	A	Scrim reinforced nonwoven needle-punched (SRNW)	Nonwoven needle-punched (NW)	4540	Needle-punched, thermally treated
GCL 3	B	Nonwoven needle-punched (NW)	Woven slit-film (W)	5260	Needle-punched
GCL 4	B	Nonwoven needle-punched (NW)	Nonwoven needle-punched (NW)	5360	Needle-punched

Table 2. Initial Properties of GCL Specimens

Test No.	GCL	Initial W/C (%)	Water Added (g)	Final M/C (%)	Base Roughness	Edge Constraint
1	GCL 1	8.1	500	55	smooth	fixed
2	GCL 1	8.1	500	55	smooth	fixed
4	GCL 2	6.6	500	60	smooth	fixed
5	GCL 2	6.6	500	60	smooth	fixed
9	GCL 3	36	500	90	smooth	fixed
10	GCL 3	36	500	90	smooth	fixed
12	GCL 4	34	500	85	smooth	fixed
13	GCL 4	24	500	70	smooth	fixed
14	GCL 4	34	500	85	smooth	free

## 5. METHODOLOGY

### 5.1 Sample Preparation

The majority of the GCL specimens (including the control tests) were cut to dimensions of 600 mm in the machine direction (MD) by 350 mm in the cross-machine direction (XD). These samples were then placed on 420mm by 620 mm aluminum baking pans. Following measurement of initial properties, the samples were clamped, in a relaxed state, to the pans by means of a 25 mm wide bar clamp. This restraint is intended to simulate conditions in the field, where GCL panels are often held down by means of an anchor trench. The total specimen area between clamps was thus 550 mm by 350 mm.

Following the methodology of Thiel et al. (2006), a 25 mm border was drawn on all sides of each GCL specimen to enable hand measurements of the dimensions of the sample whilst minimizing edge effects; this resulted in an area of interest of 500 mm by 300 mm. Measurement points were also drawn at quarter points across the sample. All final calculations were based on the distance between border lines, hereafter termed the gauge distance.

Certain specimens, which investigated the effect of differing boundary conditions on the rate and magnitude of shrinkage, were constructed with slight differences from the standard case illustrated above. On tests examining the effect of end restraint, samples were left unclamped; to allow the area of interest to remain the same as in other tests, these samples were cut to initial dimensions of 550 mm by 350 mm.

Once the sample pans were constructed, initial conditions were recorded. Each specimen was then wetted with 500g of water, bringing the samples to the final water contents shown in Table 2, by means of an 8L commercial garden sprayer. To ensure a uniform spraying technique, samples were sprayed in a back-and-forth motion, with the nozzle held approximately 50mm from the samples. The final moisture content was dependant on both the initial water content of the sample in question, as well as the amount of bentonite.

Immediately following the water application, samples were placed in a room at 20°C for hydration and moisture equilibration. To prevent moisture loss, each sample was covered with clear plastic sheeting. Following this equilibration period, which took approximately 8 hours, samples were placed in ovens at 60°C and left for 15 hours to dry; this applied heating cycle returned the samples to residual moisture content. A dummy sample was added to the ovens to confirm the effectiveness of the drying cycle. This particular drying cycle is similar to that used in previous laboratory studies by Thiel et al. (2006).

At the conclusion of the heating cycle, specimens were removed from the ovens and returned to the 20°C room. Measurements were taken at key locations on each sample; the samples subsequently underwent the wetting process as described above. Handling of samples required approximately 1 hour, resulting in a 24-hour total cycle length. The testing process was designed such that this wetting/drying cycle was repeated until such time as shrinkage ceased. The cycle is illustrated in Figure 1.

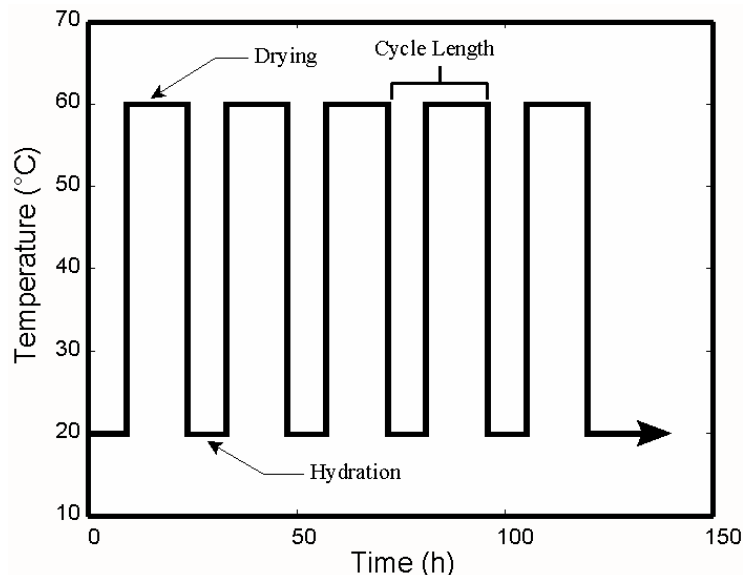


Figure 1. Hydration and Drying Cycles

## 5.2 Manual Strain Measurement

Initial shrinkage calculations were performed on the basis of daily hand measurements taken immediately following the drying portion of each cycle. The measurements were taken at the quarter points across the width of the sample; both the gauge distance and the total distance were noted. In samples which were unrestrained, measurements were also taken at the quarter points along the length of the sample, to account for shrinkage in that direction. All measurements were taken to the nearest 0.5 mm and were used to provide an independent check on the more precise measurements obtained using digital image correlation.

## 5.3 Digital Strain Measurement

Digital image correlation is an image processing technique which enables deformations to be tracked by comparing a series of digital images; in this case, images of the GCL samples at the end of each part of the shrinkage and swelling cycles. Using the code GeoPIV developed by White et al (2003), this technique was used to track the cyclic strains of the GCL samples at many locations. As shown in Figure 2, fifty-one 64x64 pixel regions of the GCL image are selected along top and bottom of the sample. Using the unique color distribution of each particular area of interest (the image texture of these patches), these locations can be found with a high degree of precision in subsequent images. Thus, the top and bottom rows of patches can be used as virtual strain gauges to calculate shrinkage strain in the cross-machine direction. Similarly samples which were unrestrained can have patches defined along their width to track strain in the machine direction. The small and unavoidable camera movements were eliminated by performing close-range photogrammetry on stationary control points on each of the pans (Figure 2).

Digital photographs were taken with a 10 megapixel digital SLR camera mounted to a specially constructed frame. Photographs were taken twice per cycle: once immediately following the drying phase (but before applying water) and at the end of the hydration period (immediately before the drying phase).

White et al. (2003) have shown that the precision of GeoPIV is typically better than  $1/10^{\text{th}}$  of a pixel (White et al., 2003). Photographs analyzed in this paper were taken at a resolution of approximately 0.18 mm per pixel. Therefore, the analysis has an approximate error of 0.018 mm. Translation of this error to that of sample strain depends on the gauge distance being measured. For measurements across the sample width (300 mm), the approximate strain error is 0.006%; for measurements across the sample length (500mm, corresponding to samples which were unrestrained), the approximate strain error is 0.004%.

## 6. RESULTS

As restrained samples were submitted to wetting and drying cycles, they began to shrink in the cross-roll direction. This is shown in Figure 2 in which the GCL has begun to curve inward near the centre of the specimen. As would be expected, the GCL shrinks least near the ends of the sample, where the clamps constrain movement; maximum shrinkage occurs near the middle. This is consistent with earlier findings (Thiel et al., 2006, Bostwick et al., 2007).

Figure 3 shows the progressive accumulation of strain in Test 1 (the same sample as is shown in the photographs of Figure 2). As testing progresses the rate of shrinkage changes, with the most rapid changes occurring in the first few cycles. In this particular test, maximum shrinkage occurs at approximately 175 mm from the left clamp. However, to permit consistent comparison between successive tests, all shrinkage below is expressed in terms of the shrinkage at midpoint. In unrestrained samples, the effect of midpoint shrinkage was not as noticeable. Samples tended to shrink in both directions, with reasonably uniform shrinkage along the sample length and width. Again, to permit comparison among samples, shrinkage was expressed as that at midpoint.

### 6.1 Effect of GCL Type

Four GCLs were investigated in this study: two with nonwoven/ nonwoven geotextiles, and two with woven/nonwoven geotextiles. For each type of GCL, two tests were completed, to provide a basis for comparison.

Figure 4 shows the shrinkage of GCL 1 with respect to the number of testing cycles. In the figure, one cycle is equal to a full 24-hour period, comprising both a wetting (lower relative value of strain) and a drying (higher relative value of strain) period. As each GCL sample is wetted, it experiences swelling (positive strain) as the water is absorbed. During the drying portion of the cycle, shrinkage occurs (negative strain) which results in a net shrinkage of the sample. When the sample is rewetted, it once again swells; however, it is unable to recover all of the shrinkage strains. The rate of shrinkage is at first rapid, and slows as the sample undergoes progressively more cycles. The cyclic strain amplitude, or difference between maximum and minimum shrinkage, also increases as testing progresses. After a period of time, the amount of maximum shrinkage becomes asymptotic, and will no longer continue to increase. In GCL 1, this occurs after approximately 18 cycles.

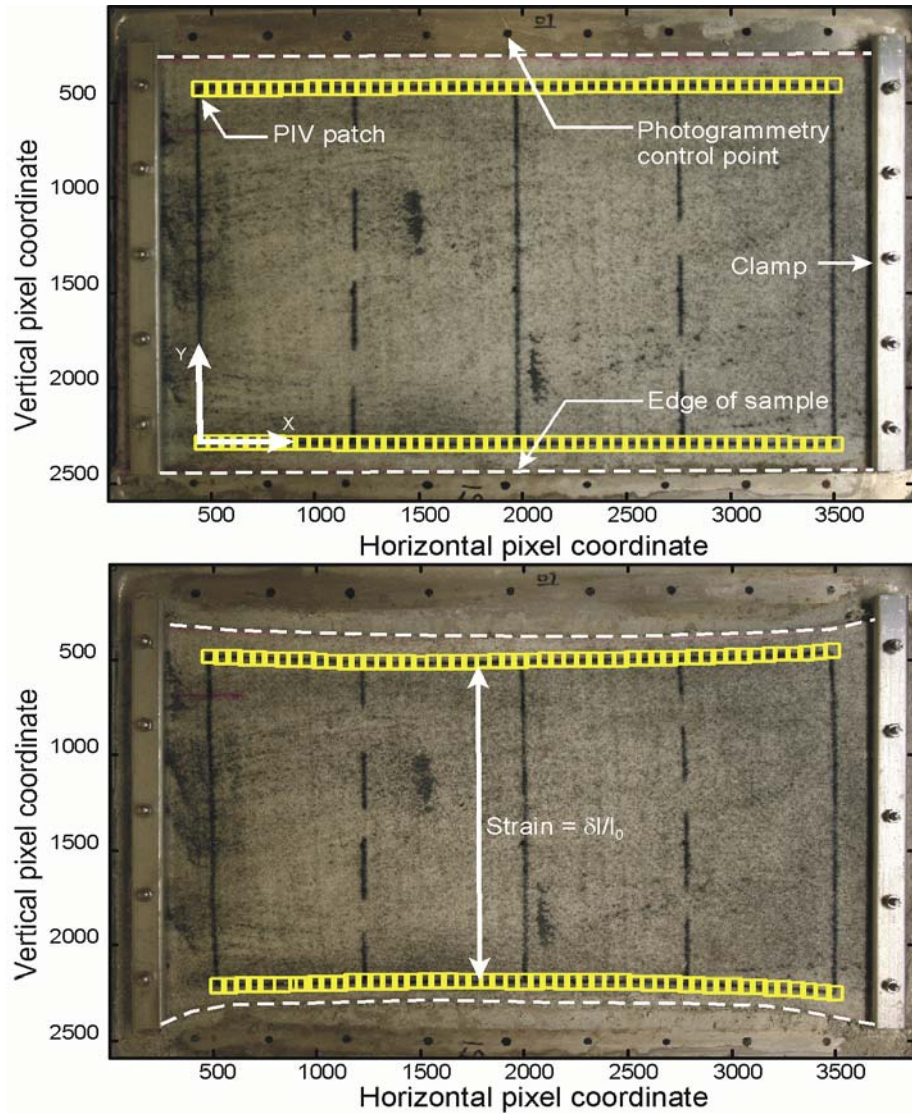


Figure 2. Measurement of shrinkage for Test 1

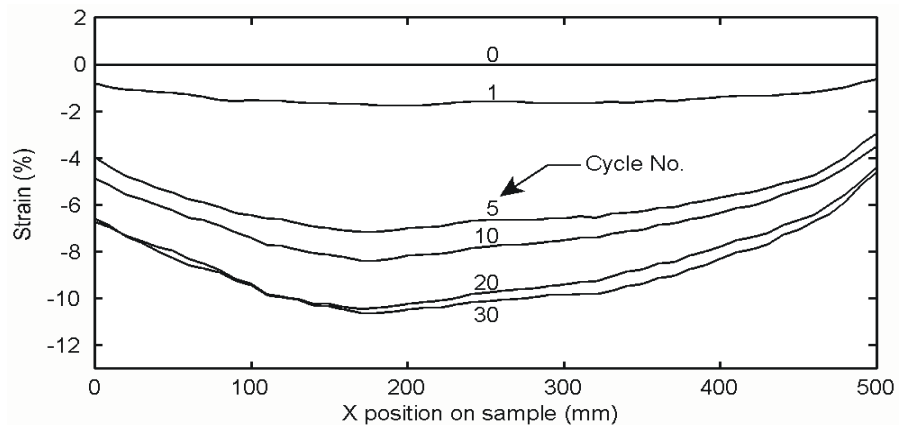


Figure 3. Variation of shrinkage strains along MD for Test 1

As can be seen in Figure 4, duplicate Tests 1 and 2 exhibited similar behavior. Both samples reached comparable shrinkage maximums of approximately 10%; the strain amplitudes of each cycle are similarly consistent. A maximum strain difference of approximately 1.5% existed between the two tests at any point in time. This could be due in part to inherent differences in the GCL between the two samples.

Figure 5 illustrates the behavior of GCL 2 for the same conditions. These two tests (4 and 5) display the same trend as the GCL 1 data, with an initial swelling followed by a net shrinkage. Again, shrinkage begins rapidly, slowing as more cycles are accumulated. However, Tests 4 and 5 did not show as close an agreement in shrinkage values as tests on GCL 1, with a difference in strain of up to 3% at times. The strain amplitudes are also dissimilar, with Test 4 showing a more marked difference between maximum and minimum shrinkage. The reason for these results is unclear; however, this data indicates that there is potential for scrim reinforcement to reduce the magnitude of shrinkage strains. Additional tests are currently underway to investigate this phenomenon. The observed dimensional stability of GCL 3, shown in Figure 6, once again shows the trends evident in the other tests, with the rate of shrinkage progressively declining as tests advance. The data for duplicate tests appears to be in agreement, with Test 9 typically experiencing 1% less strain than Test 10. The tests became reasonably asymptotic at 18 cycles; on average, the strain at this point is between 10 and 11%.

GCL 4 has, at present, undergone only a small number of wetting and drying cycles. These two tests (Figure 7) show excellent repeatability and the shape of the curve resembles typical GCL shrink/swell behavior. Further testing on these specimens must be completed to establish their full shrinkage patterns.

## 6.2 Effect of End Boundary Condition

To assess the effect of end restraint on GCL shrinkage, several samples were left unclamped at their ends. This condition allows shrinkage to occur according to the natural anisotropy of the GCL. In addition, the effect of tension, imparted in the clamped samples as they shrink, is not present in this type of test. Figure 8 shows the shrinkage of a sample of GCL 4 in both the machine (MD) and the cross-machine (XD) directions. This test follows the same pattern as the previous restrained tests. The amplitude of incremental shrinkage in the MD was found to be less than that in the XD; for this particular GCL, the ratio of incremental MD to XD shrinkage amplitude was found to be approximately 0.85. The maximum XD shrinkage for this test was found to be approximately 8.5% after 8 cycles; this is quite close to the preliminary results obtained from the restrained GCL 4 in the XD. For this product, early data suggests that shrinkage in the XD is the same for both fixed and free specimens with the aspect ratio used in these tests; however this needs to be confirmed after more cycles.

## 6.3 Comparison with Previous Results

In the present study, the maximum shrinkage strain arising from severe combined thermal and moisture cycles was found to be on the order of 10 to 12%, with this value of shrinkage occurring after approximately 18 cycles. This maximum strain magnitude is in agreement with a significant percentage of the tests conducted by Thiel et al. (2006). However, the very large strains experienced by certain specimens reported by Thiel et al. (on the order of 20%) shrinkage strain were not found in the present study. Further, Thiel et al. (2006) report that their tests did not reach an equilibrium value of strain even after 30 cycles. Further tests are currently underway to investigate these phenomena to clarify these points.

## 6.4 Comparison with Field Data

Data was obtained from the Godfrey experimental liner test site following one year of liner exposure. GCL 4 was found to have a maximum panel movement of 70mm, while GCL 2 showed a panel separation of at most 3mm. In both cases the initial overlap was 300mm and hence no panel separation had occurred for either GCL. Assuming an overall panel width of 4.7m, this corresponds to panel shrinkages of 1.5% and 0.06%, respectively. This suggests that field shrinkage, in a Canadian climate, is less than that observed in laboratory studies; it also indicates that wetting and drying cycles in field situations may be seasonal, as opposed to daily. A difference in shrinkage between the two products is also observed. Monitoring of the site will continue for at least another year.

## 7. CONCLUSION

Cyclic wetting and drying conditions simulated in this paper have been found to cause shrinkage in GCL specimens consistent with earlier tests by Thiel et al (2006). A number of samples, with differing initial conditions (such as GCL type, initial water content and edge restraint), were tested to examine their effect on potential GCL shrinkage. Results indicate that the type of GCL (NW/NW or NW/W) influences the total magnitude of shrinkage observed. The presence of a scrim reinforcement in GCL2 did result in less shrinkage in one test. The initial moisture content did not appear to affect shrinkage for the range of values tested. Field data taken following one year of liner exposure suggests that field

shrinkage in a cooler climate may be less than that noticed in laboratory tests. Further tests are currently underway to investigate the shrinkage behavior of GCLs in more detail.

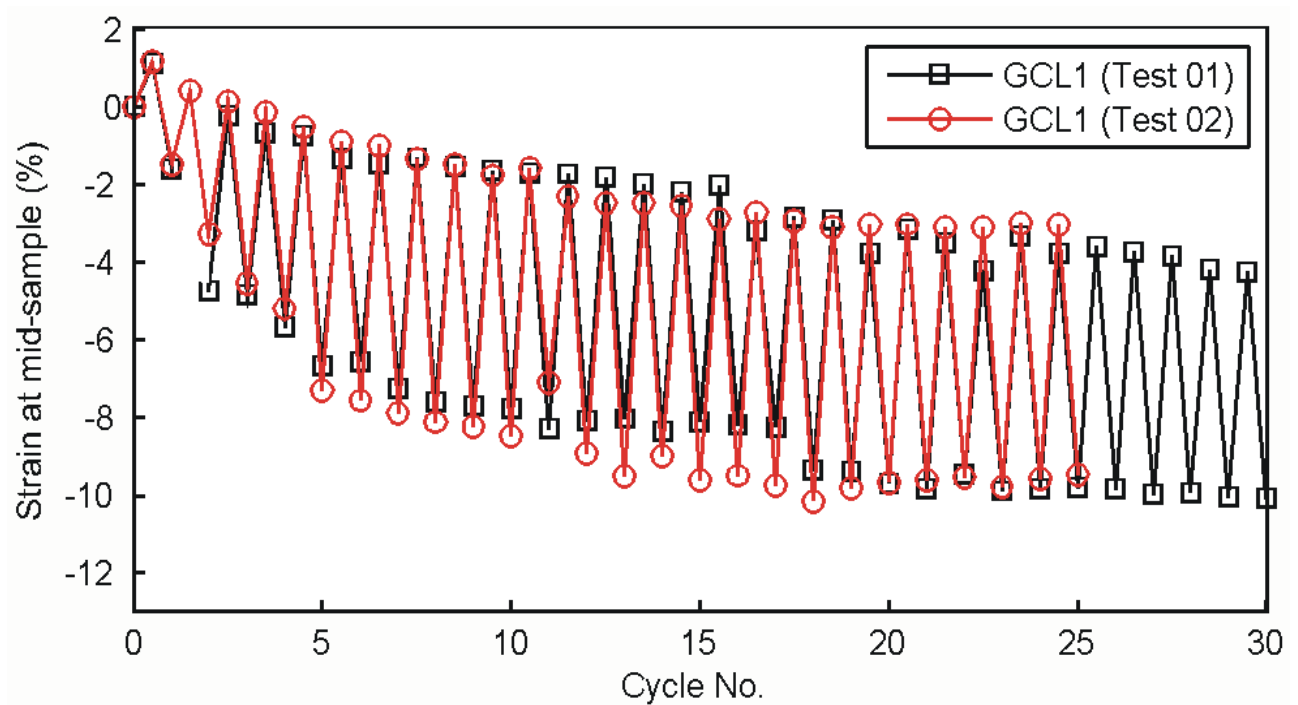


Figure 4. Strain Behavior of GCL 1

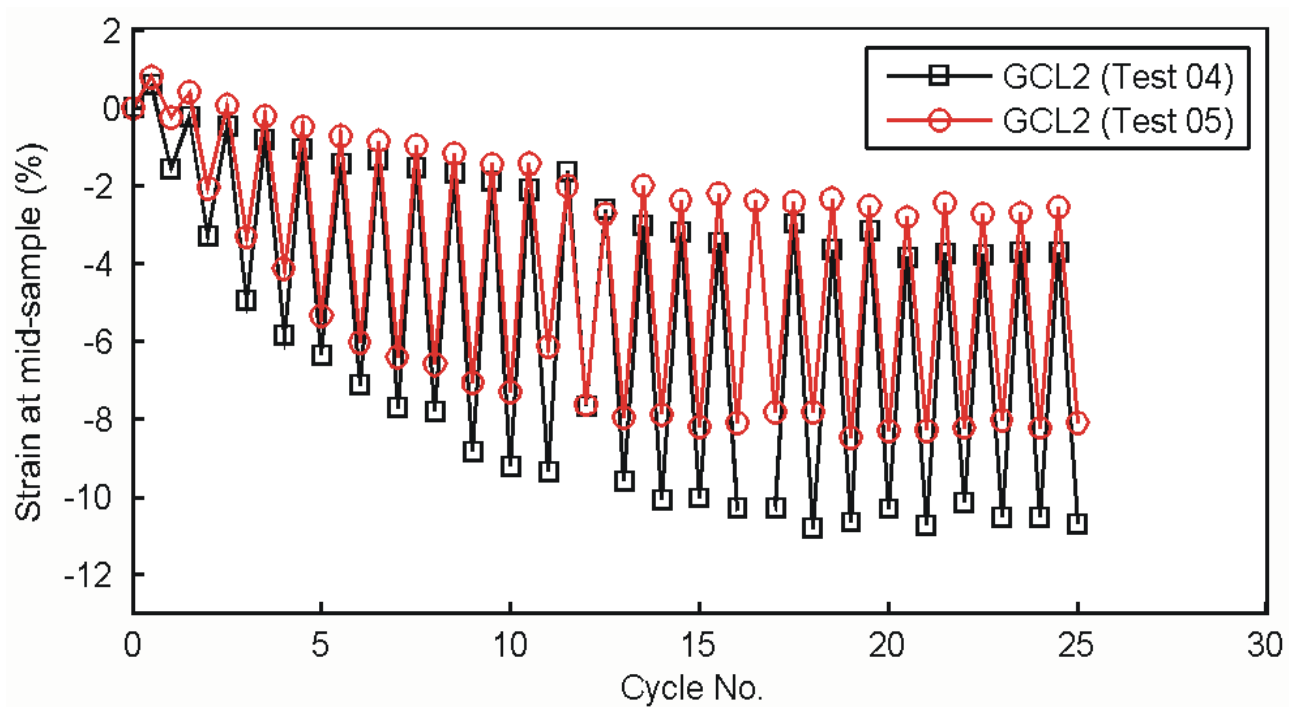


Figure 5. Strain Behavior of GCL 2

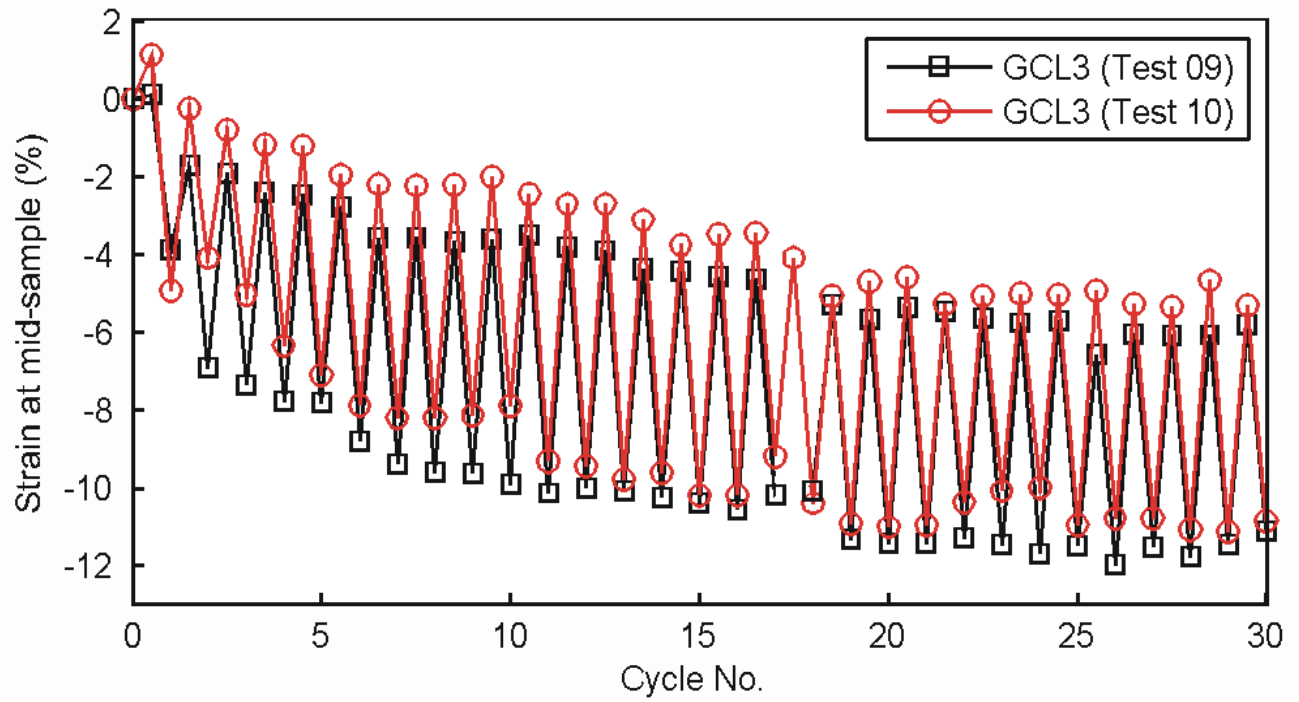


Figure 6. Strain Behavior of GCL 3

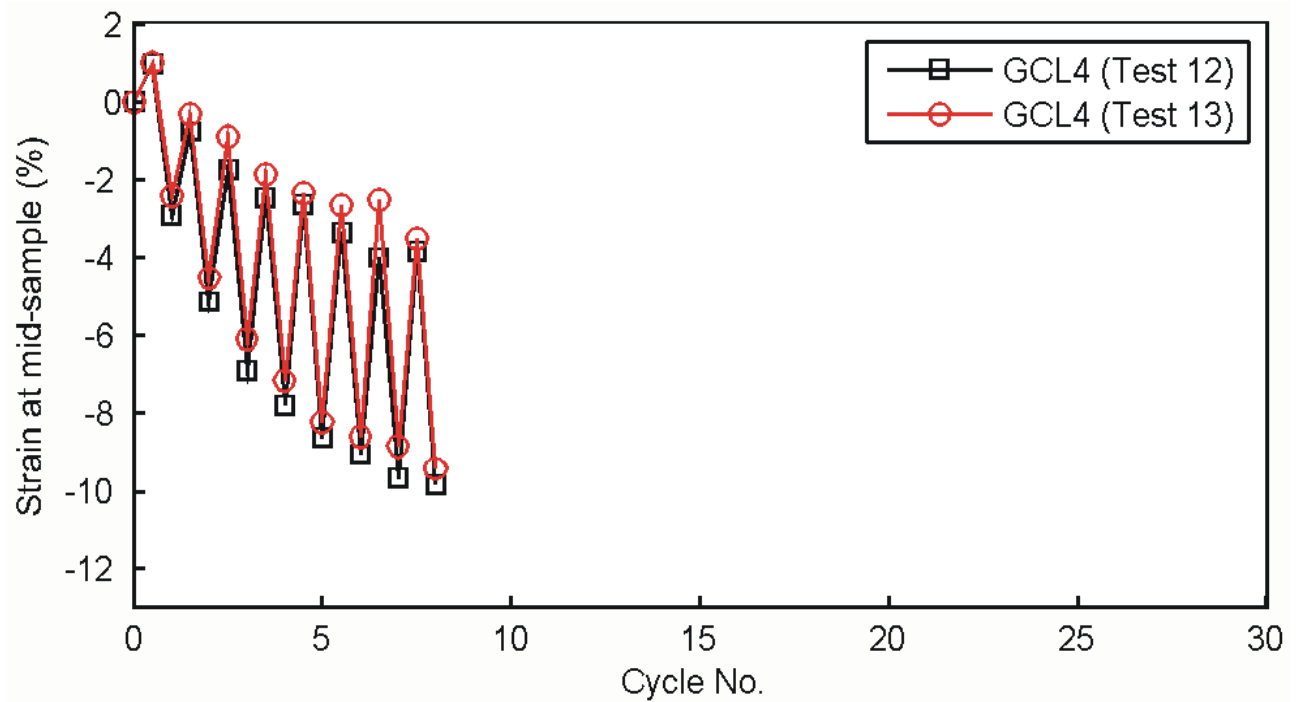


Figure 7. Strain Behavior of GCL 4

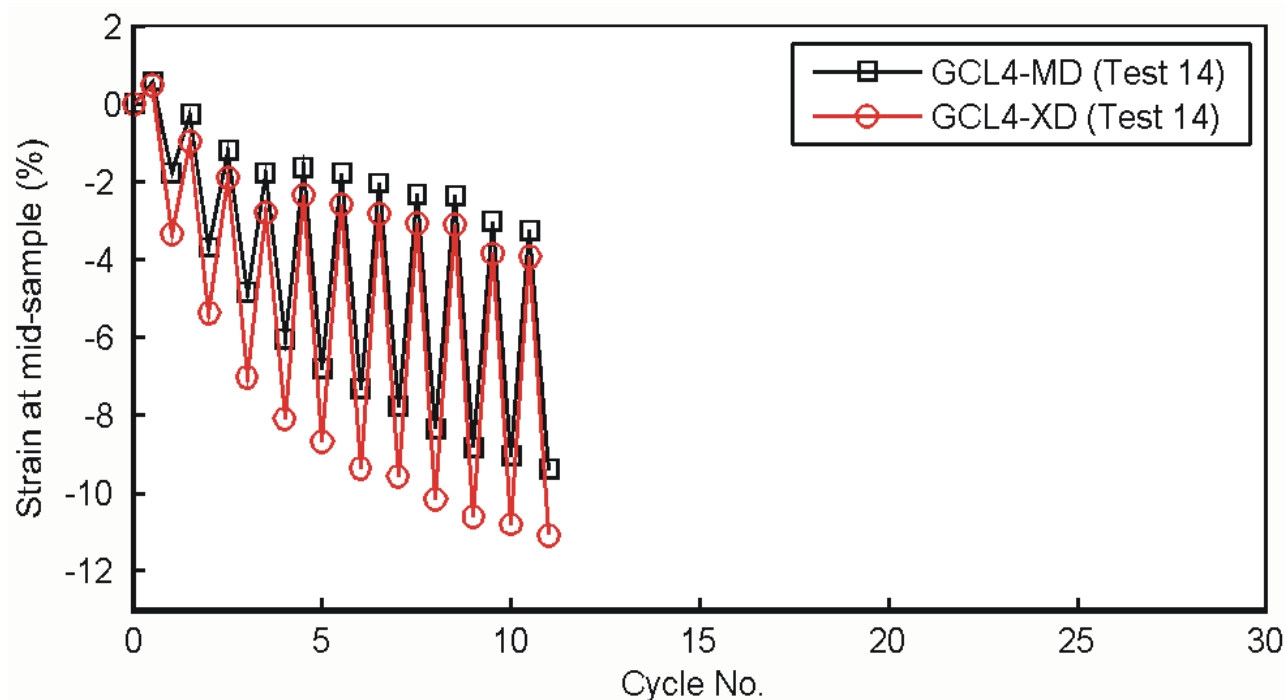


Figure 8. Strain Behavior of GCL 4, unclamped specimen

#### ACKNOWLEDGEMENTS

This study was financially supported by the Natural Science and Engineering Research Council of Canada (NSERC), the Ontario Centres of Excellence, and Terrafix Geosynthetics Inc. The authors are grateful to their industrial partners, Terrafix Geosynthetics Inc, Solmax International, Ontario Ministry of Environment, Gartner Lee Ltd, AMEC Earth and Environmental, Golder Associates Ltd., and CTT group.

#### REFERENCES

- Bostwick, L.E., Rowe, R.K., Take, W.A. and Brachman, R.W.I. (2007). The Effect of Sample Size on Shrinkage of a Non-Scrim Reinforced Geosynthetic Clay Liner, *60<sup>th</sup> Canadian Geotechnical Conference*, Ottawa, ON, 2123-2128.
- Brachman, R.W.I., Rowe, R.K., Take, W.A., Arnepalli, D.N., Chappel, M., Bostwick, L.E. and Beddoe, R. (2007). Queen's Composite Geosynthetic Liner Experimental Site, *60<sup>th</sup> Canadian Geotechnical Conference*, Ottawa, 2135-2142.
- Koerner, R.M. and Koerner, G.R. (1995). Temperature Behavior of Field Deployed HDPE Geomembranes, *Geosynthetics '95*, IFAI, Nashville, TN, USA, 3:921-937.
- Koerner, R.M. and Koerner, G.R. (2005). InSitu separation of GCL panels beneath exposed geomembranes, *Geotechnical Fabrics Report*, June-July 2005: 34-39.
- Pelte, T., Pierson, P. and Gourc, J.P. (1994). Thermal analysis of geomembranes under the effect of solar radiation, *Geosynthetics International* 1(1): 21-44.
- Rowe, R.K. (2005). "Long-term performance of contaminant barrier systems", *Geotechnique*, **55** (9): 631-678.
- Thiel, R. and Richardson, G. (2005). Concern for GCL shrinkage when installed on slopes, *JGRI-18 at GeoFrontiers*, GII Publications, Folsom, PA, USA, paper 2.31.
- Thiel, R., Giroud, J.P., Erickson, R., Criley, K. and Bryk, J. (2006). Laboratory measurements of GCL shrinkage under cyclic changes in temperature and hydration conditions, *8th International Conference on Geosynthetics*, Yokohama, Japan 1: 21-44.
- White, D.J., Take, W.A., and Bolton, M.D. (2003). Soil deformation measurement using particle image velocimetry (PIV) and photogrammetry, *Geotechnique* 53 (7): 619-63